

Studies on a low Reynolds number airfoil for small wind turbine applications

Joji WATA, Mohammed FAIZAL, Boniface TALU, Lesia VANAWALU, Puamau SOTIA and M. Rafiuddin AHMED*

Division of Mechanical Engineering, The University of the South Pacific, Laucala Campus, Fiji Islands

In contrast to large horizontal axis wind turbines (HAWTs) that are located in areas dictated by optimum wind conditions, small wind turbines are required for producing power without necessarily the best wind conditions. A low Reynolds number airfoil was designed after testing a number of low Reynolds number airfoils and then making one of our own; it was tested for use in small HAWTs. Studies using XFOIL and wind tunnel experiments were performed on the new airfoil at various Reynolds numbers. The pressure distribution, C_p , the lift and drag coefficients, C_L and C_D , were studied for varying angles of attack, α . It is found that the airfoil achieved very good aerodynamic characteristics at different Reynolds numbers and can be used as an efficient airfoil in small HAWTs.

Low Reynolds number, airfoil, small wind turbines, pressure distribution, coefficient of lift, coefficient of drag

1 Introduction

The purpose of this study is to test and analyze a new low Reynolds number airfoil created for use in small wind turbines. In contrast to larger horizontal axis wind turbines (HAWTs) that are located in areas dictated by optimum wind conditions, small wind turbines are required for producing power without necessarily the best wind conditions [1]. These locations can be urban areas where the wind maybe turbulent and obstructed by buildings and therefore weak [2] or in regions where low wind speeds are dictated by the

geographical location such as Pacific Island Countries.

An important factor that determines the efficiency of a turbine is the profile of the blade, how effectively the profile performs at various wind speeds and especially at high angles of attack that may exist locally on a wind turbine [3]. Another factor is to have effective turbine startup and performance at low wind speeds [4-6].

Blade designers employ the actual airfoil profile along the span of the blade (which is where power is produced) whereas the root is a shape between the airfoil profile and the circular section of the hub and thus does not contribute to power generation [5]. The efficiency of the rotor largely depends on the blades profile in increasing the lift to generate sufficient torque. The airfoil is one of the fundamental parts of a rotor blade design. Its purpose is to induce suction on the upper

*Corresponding author (email: ahmed_r@usp.ac.fj)

surface of the blade to generate lift. Drag is also generated perpendicular to the lift and its presence is highly undesirable. Typical aerodynamic characteristics of an airfoil used for wind turbine applications include a high C_L to C_D (L/D) ratio, a moderate to high C_L and trailing edge stall. A high L/D ratio maximizes the energy produced by the turbine as well as reducing standstill loads, and it also contribute to higher values of torque [7]. It is desirable that at favorable L/D ratios, there is maximum C_L in order to have a small sized rotor [8]. In order to maximize the power coefficient and the torque generated, the lift coefficient (C_L) and the lift to drag ratio (L/D ratio) for the airfoil must be maximized [9-10].

The C_L value at maximum L/D should be approximately within 0.2 with respect to maximum C_L value. In addition, low roughness sensitivity with respect to the maximum L/D and C_L value is desirable for optimum power production. Small wind turbines must also overcome separation bubbles associated with low Reynolds number airfoils as discussed by Lissaman [7]. Henriques and Silva [8] developed a new high lift airfoil characterized to work well within the urban environment using XFOIL. Cencelli [11] presented the design of airfoils at different radial distances along the blade for small wind turbines designed to operate below 7 m/s wind speed.

The present work deals with the design and the parameters associated with blade geometry of a new low Reynolds number airfoil developed for small wind turbines. Low Reynolds numbers are used because of low wind speeds in pacific countries. The new airfoil was developed based on existing low Reynolds number airfoil studies through xfoil. A new airfoil was created after modifying a number of geometries, and tested in XFOIL to evaluate their aerodynamic characteristics before conducting wind tunnel tests on the final modified airfoil.

2 Methodology

a) Airfoil Design and XFOIL Testing

In the design and optimization process, a number of airfoils were selected based on their performance and the coordinates of their geometries were combined to create new airfoils. The SG6043 airfoil was combined with: GOE 15, Eppler 422, Eppler 560, and S1223. The airfoils were tested in XFOIL at $Re = 38000$, 128000 , and 205000 . The C_L vs α graphs for the tested airfoils at $Re = 38000$ and $Re = 205000$ are shown in Figure 1. The airfoil that displayed favorable C_L and L/D ratio is SG6043_Eppler 422. It has a maximum thickness of 14%, camber of 6.9% and leading edge radius of 1.18%. The geometry of the new airfoil is shown in Figure 2.

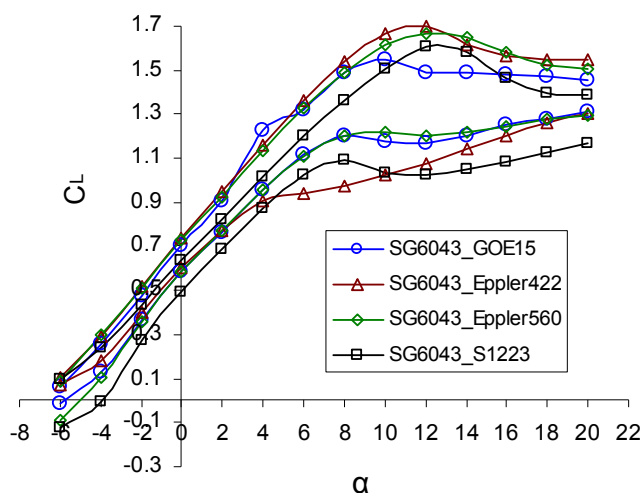


Figure 1 The C_L of the tested airfoils against α for $Re = 38000$ and $Re = 205000$.

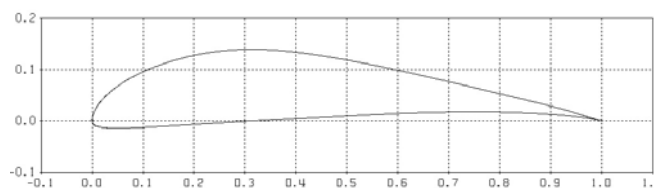


Figure 2 The geometry of the new airfoil (SG6043_Eppler 422)

The new airfoil was initially tested in XFOIL to predict its aerodynamic performance. The following parameters were used as an initial evaluation in XFOIL:

- The number of panel nodes used was set at 240
- The amplification ratio was set at 2.5 resulting in a turbulence level of 1.052%
- Viscous acceleration was set to 0
- The turbulence level was set to reflect the turbulence level in the wind tunnel.

The airfoil was then tested at different angles of attack (α) from 0 to 25° and Reynolds numbers (Re) of 20000, 27000, 38000, 128000 and 205000. The C_L vs α , L/D vs α and lift-drag polars were plotted. After the initial XFOIL test, the model airfoil was fabricated and tested in the wind tunnel.

b) Model Airfoil

Three airfoil models were made for wind tunnel experiments. Two of these airfoils were used for separate top and bottom surface pressure measurements and the third was

used for lift and drag measurements by a dynamometer. Each airfoil has a chord length of 80 mm and a span of 300 mm. The lower chord length ensured low solid blockage in the wind tunnel at high α . A total of 26 pressure taps on the bottom surface and 27 pressure taps on the top surface of the airfoil were provided. Pressure measurements were taken using two digital Furness Controls FC0510 micro-manometers with pressure ranges up to 200 mm and 2000 mm of water. The lower range manometer was used at low Reynolds numbers and the higher range manometer for higher Reynolds numbers. A 5 second time averaged pressure reading was taken for each pressure tap.

c) Lift and Drag measurements

The third airfoil model was fitted with attachment to allow the model to be connected to the dynamometer that measured C_L and C_D . The dynamometer was calibrated against known weights to measure lift and drag in kgf. The lift and drag forces were obtained by multiplying the readings with the gravitational constant.

d) Wind Tunnel Testing

The experiments were performed on an Engineering Laboratory Design (ELD) Inc. made open circuit wind tunnel in the Thermo fluids laboratory at the University of the South Pacific. The test section measured 0.3m x 0.3m in cross-sectional area and 1 meter in length. The wind tunnel is subsonic and the maximum free stream velocity attainable is 48.77m/s. The free stream velocity is set via a remote operated control unit that gives a velocity resolution of 0.08m/s. The flow velocity within the test section was corrected and set via a traversing pitot-static tube connected to a digital micro manometer. The airfoils were tested from $\alpha = -5^\circ$ to $\alpha = 25^\circ$ at Re 38000, 128000, 205000 and 257000. The results of the tests are presented in the following section.

3 Results and Discussion

a) XFOIL Results

Figure 3 shows the C_L vs α graphs at different Re. At low Re of 20000 to 38000, the C_L values generally increased to a value of 1.4 at $\alpha = 25^\circ$. A maximum C_L value of 1.7 occurs at Re 205000 at $\alpha = 12^\circ$. The higher Re (128000 and 205000) C_L curves show a gradual decline to an almost constant C_L after $\alpha = 12^\circ$. The gradual decline is an indication of trailing edge stall, which is one of the desired characteristics of an airfoil for wind turbine applications.

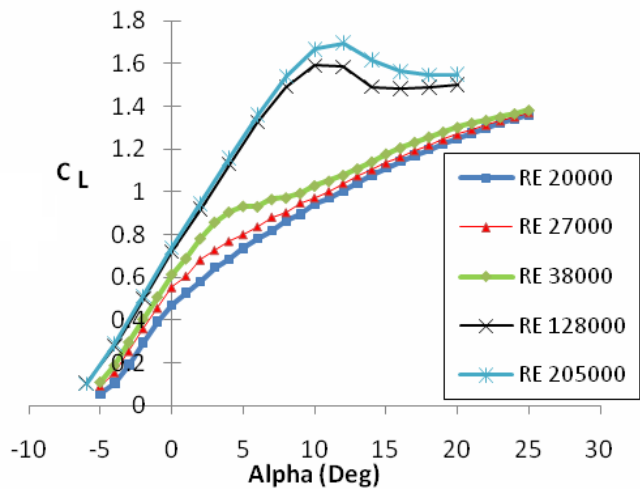


Figure 3 C_L vs α graph for the airfoil

Figure 4 shows the L/D ratio vs α plotted for the airfoil. The maximum L/D ratio is close to 80 for $\alpha = 8^\circ$. The corresponding C_L is 1.54. At maximum C_L , the L/D value is found to be 47.5. It was observed that C_L at $\alpha = 8^\circ$ was within 0.2 of the maximum C_L value and that the airfoil attained a high L/D ratio. After the initial XFOIL testing, the model airfoil was tested in the wind tunnel.

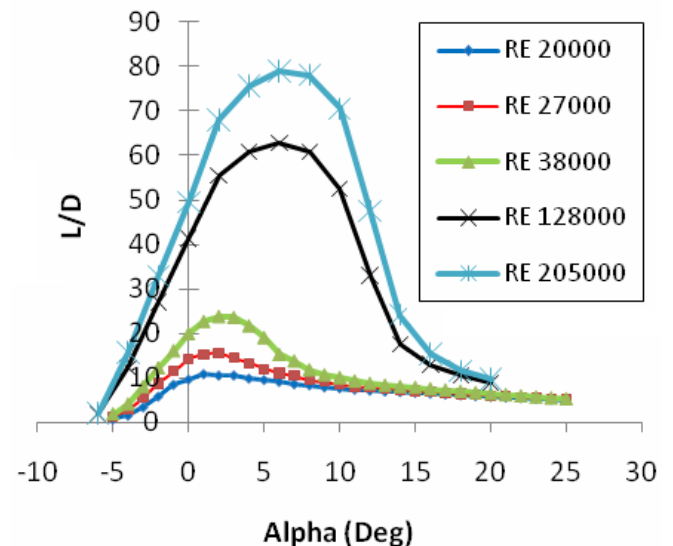


Figure 4 L/D vs α for the airfoil.

The Lift-Drag polar plot is shown by Figure 5. For $Re = 128000$ and 205000 , the lift increases considerably without much changes in C_D .

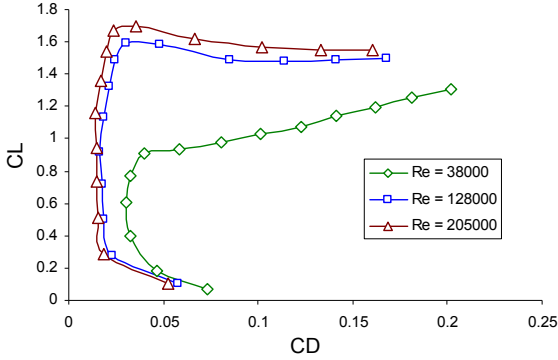


Figure 5 The Lift-Drag polar plot for the new airfoil (XFOIL results)

b) Experimental Results

Pressure measurements, C_L and C_D measurements were conducted in the wind tunnel and some of the results are presented and discussed in this section.

The C_L vs α graphs for the airfoil at different Re are shown in Figure 6. At $Re = 38000$, the C_L values are generally increasing to about 0.8 at $\alpha=22^\circ$. At this Reynolds number, the airfoil shows trailing edge stall characteristics. At Re of 128000, the C_L values showed slightly higher values from $\alpha = -5^\circ$ until $\alpha = 4^\circ$. However, the C_L continuously increased to a value of 0.9 at 22° . At higher Re of 205000 and 257000, the C_L values are increasing to a maximum value of about 1.6 and 1.7 respectively at $\alpha=15^\circ$ before dropping due to flow separation from the upper surface (trailing edge stall).

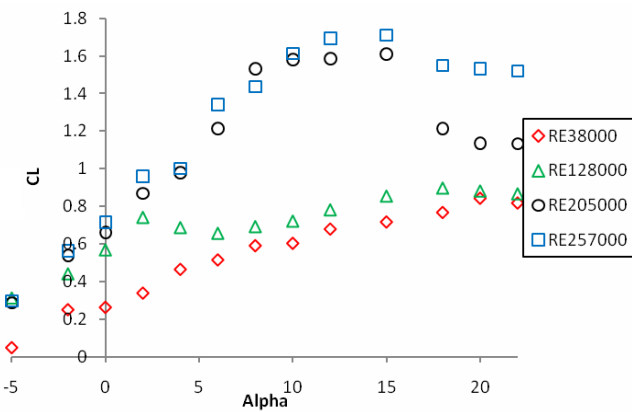


Figure 6 The experimental values of C_L vs α at different Re for the airfoil.

Comparing Figure 6 with Figure 3, the C_L for higher Re is similar. The C_L at lower Re is higher from XFOIL results than the experimental results. Pressure distributions on the surface of the airfoil are presented in Figures 7 to 11. The non-dimensionalised coefficient of pressure (C_p) is plotted against non-dimensional chord length, x/c .

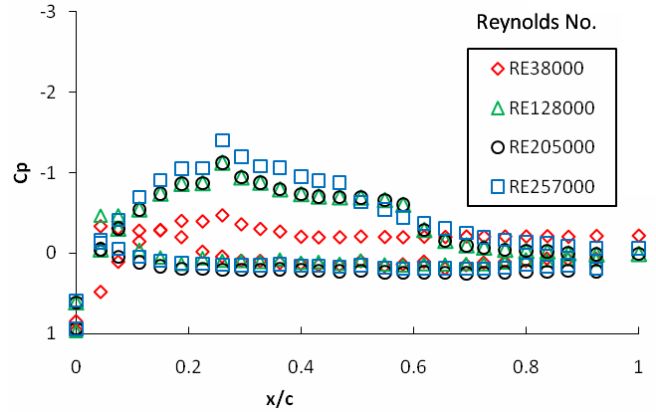


Figure 7 Pressure distribution on surface of the airfoil at $\alpha = 0^\circ$.

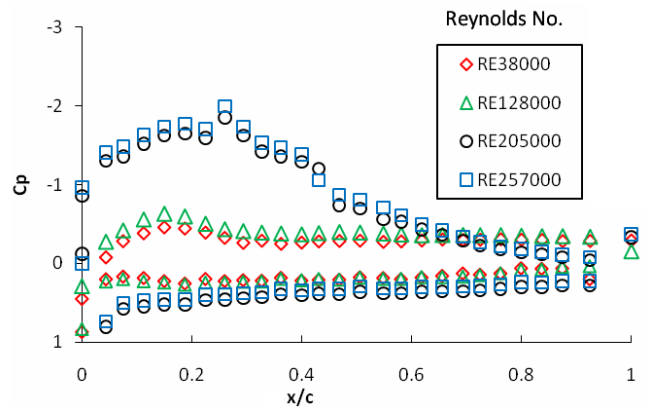


Figure 8 Pressure distribution on the surface of the airfoil at $\alpha=6^\circ$

Pressure distributions (Fig. 7) for $\alpha = 0^\circ$ and $Re 38000$ show a small pressure difference between the upper and lower surfaces. The pressure difference at this point is very small and agrees with the low C_L value plotted in Figure 6. As the angle of attack (α) is increased, the pressure difference increases (Figure 8-11) which explains the general increase in C_L presented in Figure 6. At $Re = 128000$, the pressure difference is higher compared to $Re = 38000$. The higher pressure difference results in higher C_L values plotted in Figure 6. At high angles of attack at low Re , the suction peak reduces, as can be seen from Figs. 9-11. This results in

generally lower values of C_L for these Reynolds numbers compared to higher Re.

At higher Re (205000 and 257000), the suction peak moves towards the leading edge as the angle of attack is increased; at the same time, its magnitude increases. For these Re, the flow stays attached to the surface to about $x/c = 0.7$ (Figs. 7 and 8). The gradual increase in C_L to the stall angle of $\alpha = 15^\circ$ coincides with the movement of the separation point from the location of $x/c = 0.7$ to about $x/c = 0.4$ at $\alpha = 15^\circ$ for both these Reynolds numbers (Figs. 9 and 10). The pressure difference continues to increase as the angle of attack is increased.

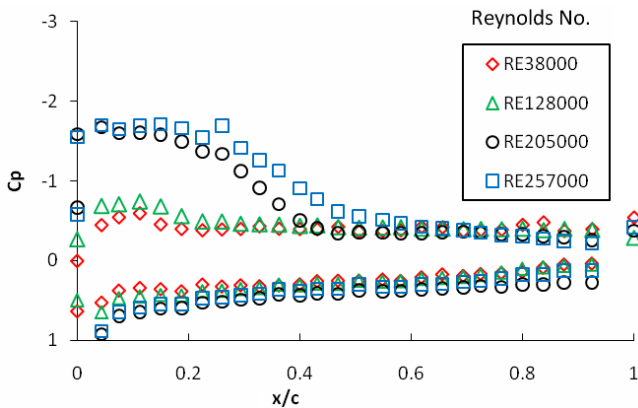


Figure 9 Pressure distribution on the surface of the airfoil at $\alpha = 10^\circ$.

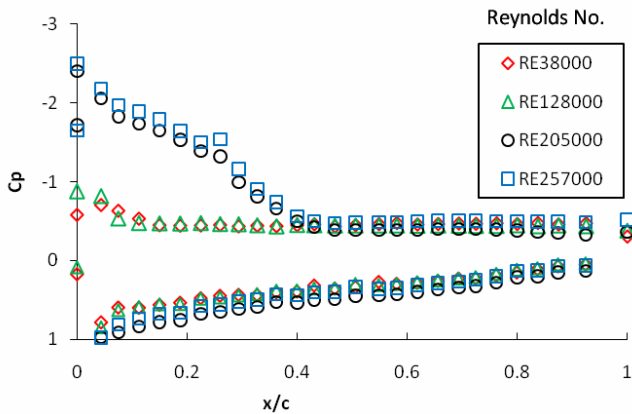


Figure 10 Pressure distribution on the surface of the airfoil at $\alpha = 15^\circ$.

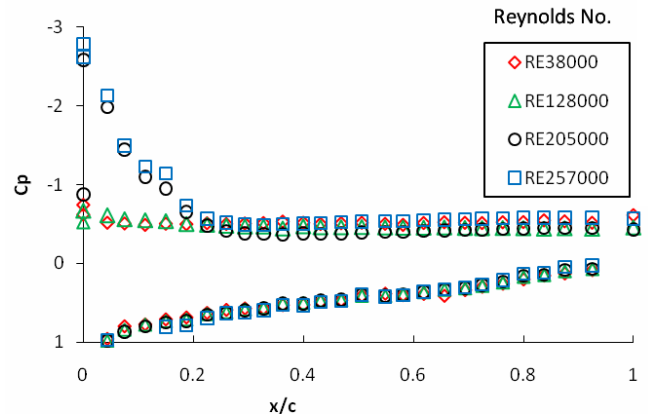


Figure 11 Pressure distribution on the surface of the airfoil at $\alpha = 22^\circ$.

Figure 11 shows the pressure distribution at $\alpha = 22^\circ$. At lower Re, the pressure on the upper surface is nearly constant, indicating early flow separation. The pressure distribution and C_L vs. α graph (Fig. 6) are in agreement with the pressure distributions showing upstream movement of the point of separation from the trailing edge as the angle of attack (α) of the airfoil is increased.

The suction peak for the higher Re of 205000 and 257000 is much higher compared to the lower Re, as shown in the pressure distributions above. Low Re flows has low energy compared to high Re flows, therefore the flow separates early in low Re flows and the lift is thus lower. At very low Re, the airfoils are known to give poor C_L to C_D ratios as reported by Lissaman [7]. The pressures on the lower surface are generally increasing with increasing angle of attack, and the stagnation point is moving to the lower surface away from the leading edge, as can be seen from Fig. 7 to Fig. 11. However, since the region close to the hub is not expected to contribute much to the rotation of the turbine blade, the poor performance is not of much concern. At higher Re, which is expected near the tip region, the performance of the airfoil is found to be good and the C_L is not dropping much as can be seen for $Re = 257000$ from Fig. 6.

Conclusions

The present work involved the creation of a new low Reynolds number airfoil from existing airfoil geometries using XFOIL. The airfoil was tested using XFOIL and also wind tunnel testing was performed to evaluate the aerodynamic characteristics of the airfoil at low Reynolds numbers. The numerical results agreed well with experimental results at higher Reynolds numbers, giving C_L values close to

1.7. Experimentally, the pressure distributions showed a stalling angle of 15° . The maximum L/D ratio is obtained at $\alpha = 8^\circ$, which can be chosen as the design angle of attack. Experimental and XFOIL results generally show good agreement with each other.

1. Ozgener O, Ozgener L. Exergy and reliability analysis of wind turbine systems: A case study, *Journal of Renewable and Sustainable Energy Reviews*, 2007, 11:1811-1826
2. Wang F, Bai L, Fletcher J, Whiteford J. The methodology for aerodynamic study on a small domestic wind turbine with scoop, *Journal of Wind Engineering and Industrial Aerodynamics*, 2008, 96:1-24.
3. Hansen M O L. *Aerodynamics of Wind Turbines*, 2nd ed. Earthscan, London, 2008.
4. Wright A K, Wood D H. The starting and low wind speed behaviour of a small horizontal axis wind turbine, *Journal of Wind Engineering and Industrial Aerodynamics*, 2004, 92:1265-1279.
5. Habali S M, Saleh I A. Design and testing of small mixed airfoil wind turbine blades. *Renewable Energy*, 1995, 6:161-169.
6. Mayer C, Bechly M E, Hampsey E, Wood D H. The starting behaviour of a small horizontal-axis wind turbine, *Journal of Renewable Energy*, 2001, 22:411-417.
7. Lissaman P B S. Low-Reynolds-number airfoils, *Annual Review of Fluid Mechanics*, 1983, 15:223-239.
8. Henriques J C C, Marques da Silva F, Estanqueiro A I, Gato L M C. Design of a new urban wind turbine airfoil using a pressure-load inverse method, *Journal of Renewable Energy*, 2009; 34:2728-2734.
9. Selig M S, Guglielmo, J J. High-Lift low Reynolds number airfoil design, *Journal of Aircraft*, 1997, 34: 72-79.
10. Van Rooij R P J O M, Timmer W A. Roughness sensitivity considerations for thick rotor blade airfoils, *AIAA Paper 2003-0350*.
11. Cernaelle N A. Aerodynamic optimization of a small scale wind turbine blade for low speed conditions, Master's Thesis, University of Stellenbosch, 2006.